Proceedings of the Second International Conference on Press-in Engineering 2021, Kochi, Japan – Matsumoto et al (eds)

An investigation into vertical capacity of steel sheet piles installed by the Standard Press-in method

K. Toda & Y. Ishihara
Giken LTD, Kochi, Japan

ABSTRACT: Steel sheet piles have long been used for temporary retaining structures. Nowadays, they are increasingly applied to non-temporary structures, but the number of load tests on sheet piles conducted so far is limited, and methods of estimating vertical and horizontal performance of sheet piles have not been well developed, possibly leading to some conservatism in design of sheet piles. Accumulation of load test results on sheet piles is essential for understanding the performance of sheet piles and rationalizing their design method. This paper focuses on sheet piles installed by Standard Press-in, and introduces three cases of static vertical load tests conducted in the field, which are collected from published sources. The results were used for back-analyzing the values of coefficients in an SPT-based design method. As a result, it was found out that the total capacity of the sheet pile can be safely estimated.

1 INTRODUCTION

Steel sheet piles have long been used for temporary retaining structures. Nowadays, they are increasingly applied to non-temporary structures such as coastal levees (Ishihara *et al.*, 2020a), railway bridge foundations (Kasahara *et al.*, 2018), stress cut-off walls (Tanaka *et al.*, 2018), liquefaction countermeasures for buildings (Kato *et al.*, 2014) and so on. However, the number of load tests on sheet piles conducted so far is limited, and methods of estimating vertical and horizontal performance of sheet piles have not been well developed, possibly leading to some conservatism in design of sheet piles. Accumulation of load test results on sheet piles is essential for understanding the performance of sheet piles and rationalizing their design method.

This paper introduces results of static vertical load tests on sheet piles installed by Standard Press-in (a press-in technique that does not use the installation assistance such as water jetting or augering but may use the technique of repeated penetration and extraction (surging)) from published sources as well as from our original experiments, and attempts to make modifications in an existing SPT-based design method based on the collected load test results.

2 COLLECTING INFORMATION ON STATIC LOAD TESTS ON SHEET PILES INSTALLED BY STANDARD PRESS-IN

2.1 *Is20 test series: U-shaped 400-millimeter-wide sheet pile (SP-III) in soft ground layered by clay and sand*

The first case was taken from a published source (Ishihara *et al.*, 2020b). As shown in Figure 1, the ground consists of soft alluvial soils. A relatively hard layer of fine sand, with SPT N exceeding 10 at the depth (z) from 5.5m to 9m, was sandwiched by soft layers of silty sand and silty clay. As shown in Figure 2, a total of 14 U-shaped sheet piles with the width of 400mm (SP-III) were installed by Standard Press-in, based on the press-in conditions summarized in Table 1. Piles No. 2, 5, 6, 9 and 10 were load tested by a simplified test method using the press-in machine, with different time after the end of installation (t_{LT}).

As shown in Figure 3, the set-up ratio increased linearly with t_{LT}. The greater values of No. 5, 9 compared than No. 6, 10 is thought to be due to the effect of the existence of piles in both sides of the test piles during the load test.

In this test series, the sheet piles were not instrumented with strain gauges. Instead, pull-out tests were conducted immediately after the compressive

DOI: 10.1201/9781003215226-13

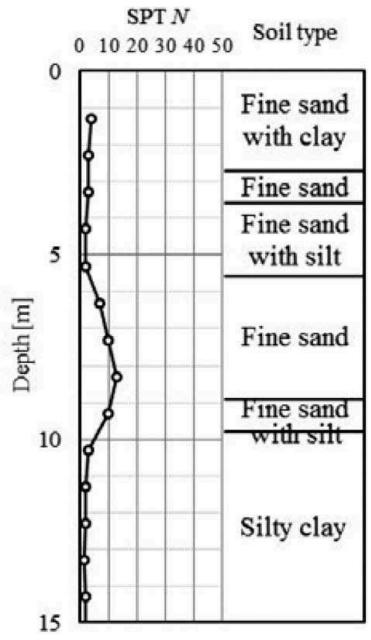

Figure 1. Site profile (Is20 test series).

load test, and the pull-out resistance during the pull-out test was assumed to be equal to the shaft resistance during the compressive load test. The base capacity (Q_{bf}) and the shaft capacity (Q_{sf}) were defined as the values recorded when the pile head displacement reached $0.1D_{o,eq}$, where $D_{o,eq}$ is the outer diameter of an imaginary tubular pile that has the same areas of the annulus and the hollow part of the pile as shown in Figure 4 (IPA, 2017). As a result, the base capacity (Q_{bf}) and the shaft capacity (Q_{sf}) of pile No. 10 was estimated to be 140kN and 140kN respectively, as summarized in Table 2.

2.2 *Om19 test series: Hat-shaped 900-millimeter-wide sheet pile (SP-50H) in soft ground layered by sand and silt*

The second case was taken from another published source (Omura *et al*., 2019). As shown in Figure 5, the ground consists of soft sand layer and a soft sandy silt layer underlaying the sand layer. Hat-shaped sheet piles with the width of 900mm (SP-50H) were used as test piles. As shown in Figure 6, three test piles (A-1, A-2, A-3) were installed by Standard Press-in and then load tested, without their interlocks being connected to the adjacent pile. The other piles were installed by a vibro-hammer method and were used as reaction piles during press-in piling.

The test piles were instrumented with axial strain gauges and a measurement device for the base displacement, as shown in Figure 5. Q_{bf} and Q_{sf} were defined as the values recorded when the pile base displacement reached $0.1W_{sp}$, where W_{sp} is the width of the sheet pile. Q_{bf}, Q_{sf} and the unit shaft capacity are summarized in Table 3.

2.3 *Eg21 test series: U-shaped 600-millimeter-wide sheet pile (SP-IIIw) in soft ground layered by sand and silt*

The third case was our original experiment. As shown in Figure 7, the ground consists of soft alluvial silt with SPT N values being smaller than 5, underlain by a relatively hard (but still soft) silty sand and gravel layer with SPT N values exceeding 10. The test pile was a U-shaped sheet pile with the width of 600mm (SP-IIIw), and was instrumented with axial strain gauges as shown in Figure 8.

The test layout is shown in Figure 9. The test pile was installed by Standard Press-in based on the press-in conditions summarized in Table 4, using a press-in machine (F201) which was grasping the piles No. A, B, C and D. Pile A was very short and had been welded to the pile B, without being embedded into the ground. The other piles (B, C, D) were embedded by 6.4m.

Figure 10 shows the load displacement curves obtained in the load test. Q_{bf} and Q_{sf}, determined as the values at the pile head displacement of $0.1D_{o,eq}$, are summarized in Table 5.

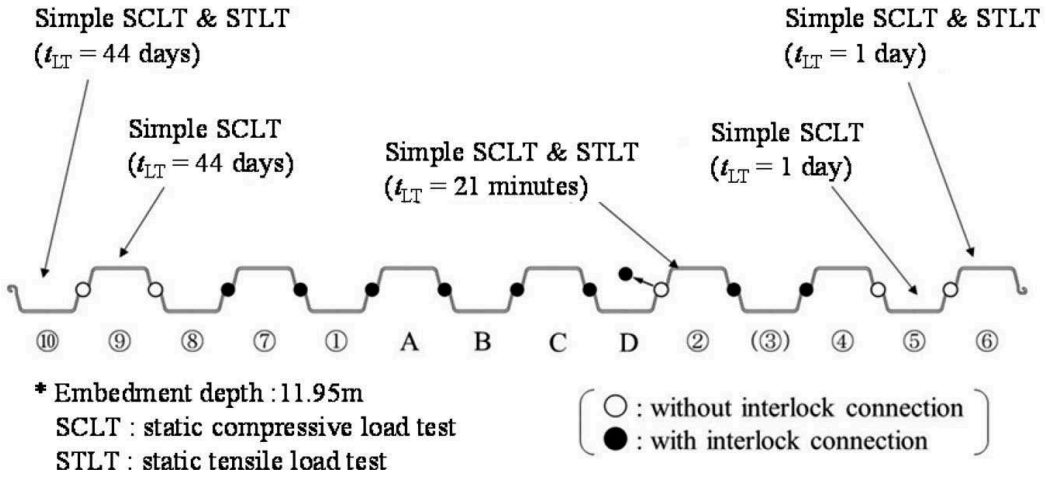

Figure 2. Layout of the field test (Is20 test series) (after Ishihara *et al*., 2020).

Table 1. Test conditions (Is20 test series).

(a) Press-in piling.					(b) Load test.		
Pile No.	Displacement of penetration and extraction (l_d and l_u) [mm]	Rate of penetration and extraction [mm/s]	Interlock connection	Press-in machine (WC in kN)	Pile No.	Tensile loading history	Curing period t_{LT}
2	l_d=400, l_u =200	30	None	F111 (19.7)	2	None	21 mintues
5	l_d=400, l_u =200	30	None	F111 (19.7)	5	Yes	1 day
6	l_d=400, l_u =200	30	None	F111 (19.7)	6	None	1 day
9	l_d=400, l_u =200	30	None	F111 (19.7)	9	Yes	44 days
10	l_d=400, l_u =200	30	None	F111 (19.7)	10	None	44 days

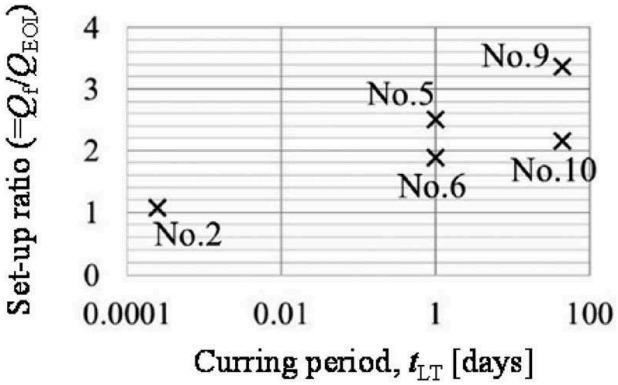

Figure 3. Effect of curing period on pile capacity (Ishihara *et al*., 2020).

3 SPT-BASED DESIGN METHODS FOR VERTICAL CAPACITY OF SHEET PILES INSTALLED BY STANDARD PRESS-IN

3.1 *Existing SPT-based design methods in Japan*

In this sub-section, two SPT-based methods to estimate Q_{bf} and Q_{sf} of piles installed by Standard Press-in will be introduced.

The first one is what has been used in the field of roads in Japan (JRA, 1999). In this method, Q_{bf} is estimated by:

$$Q_{bf} = q_{bf} \times A_{bp} \quad (1)$$

Type of sheet pile	$A_{o,eq}$ [m^2]	$A_{i,eq}$ [m^2]	$D_{o,eq}$ [m]	$D_{i,eq}$ [m]
SP-III	0.007642	0.043496	0.2552	0.2353
SP-IIIw	0.010390	0.090971	0.3593	0.3403
SP-10H	0.011000	0.106836	0.3873	0.3688

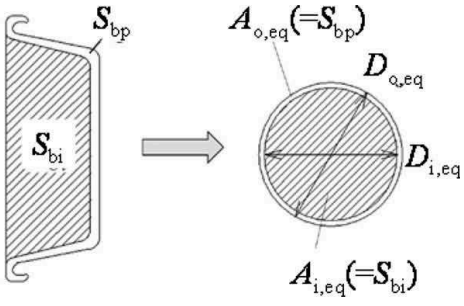

Figure 4. The outer diameter of an imaginary tubular pile (IPA, 2017).

Table 2. Summary of the load test results (Is20 test series).

Pile No.	Curing period t_{LT}	End of installation capacity Q_{EOI} [kN]	Total capacity Q_f [kN]	Base capasity Q_{bf} [kN]	Shaft capasity Q_{sf} [kN]	$\frac{Q_f}{Q_{EOI}}$
2	21 minutes	150	160	70	90	1.07
5	1 day	100	250	-	-	2.50
6	1 day	120	25	100	125	1.88
9	44 days	110	370	-	-	3.37
10	44 days	130	280	140	140	2.15

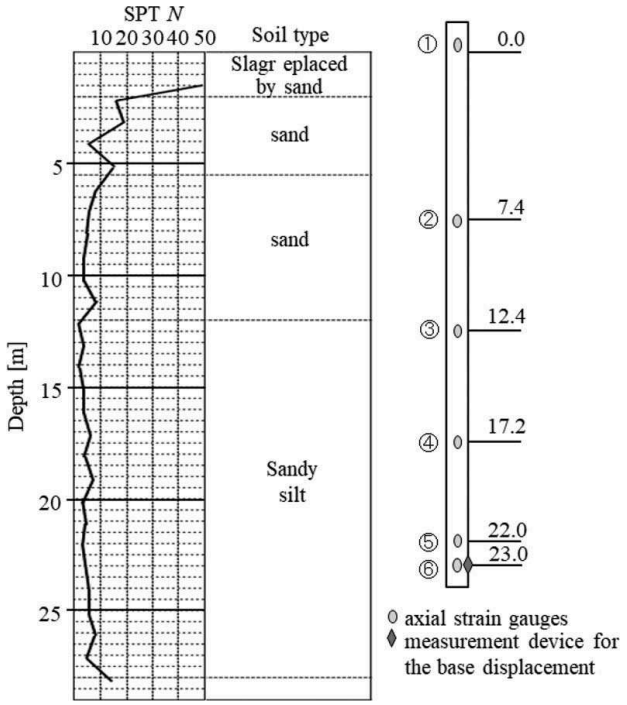

Figure 5. Site soil profile, and distribution of strain gauges and measurement device (Om19 test series) (after Omura *et al*., 2019).

where q_{bf} is the unit base resistance obtained by Eq. (2) and A_{bp} is the net cross-sectional area of the pile.

$$q_{bf} = \begin{cases} \min(200 \times N_{D1}, 8000) & \text{[kPa] (for sand)} \\ - & \text{[kPa] (for clay)} \end{cases} \tag{2}$$

Here, N_{D1} is the SPT N value averaged from 0 to 2 meters above the pile base. On the other hand, Q_{sf} can be estimated by:

$$Q_{sf} = \int (q_{sf} \times W_{sp}) dz \tag{3}$$

where q_{sf} is the unit shaft resistance obtained by Eq. (4) and z represents the depth.

$$q_{sf} = \begin{cases} \min(2 \times N, 100) & \text{[kPa] (for sand, } N > 2) \\ \min(10 \times N, 150) & \text{[kPa] (for clay, } N > 2) \\ 0 & \text{[kPa] (for, } N \leqq 2) \end{cases} \tag{4}$$

The second one is what has been used in the field of railways in Japan (RTRI *et al*. 2014). In this method, Q_{bf} is obtained by Eq. (1), in which q_{bf} is estimated by:

$$q_{bf} = \begin{cases} \min(210 \times N_D 2, 10000) & \text{[kPa] (for sand)} \\ - & \text{[kPa] (for clay)} \end{cases} \tag{5}$$

where N_{D2} is the smallest SPT N value from 0 to 3 meters below the pile base. On the other hand, Q_{sf} is estimated by:

$$Q_{sf} = \int (q_{sf} \times P_{sp}) dz \tag{6}$$

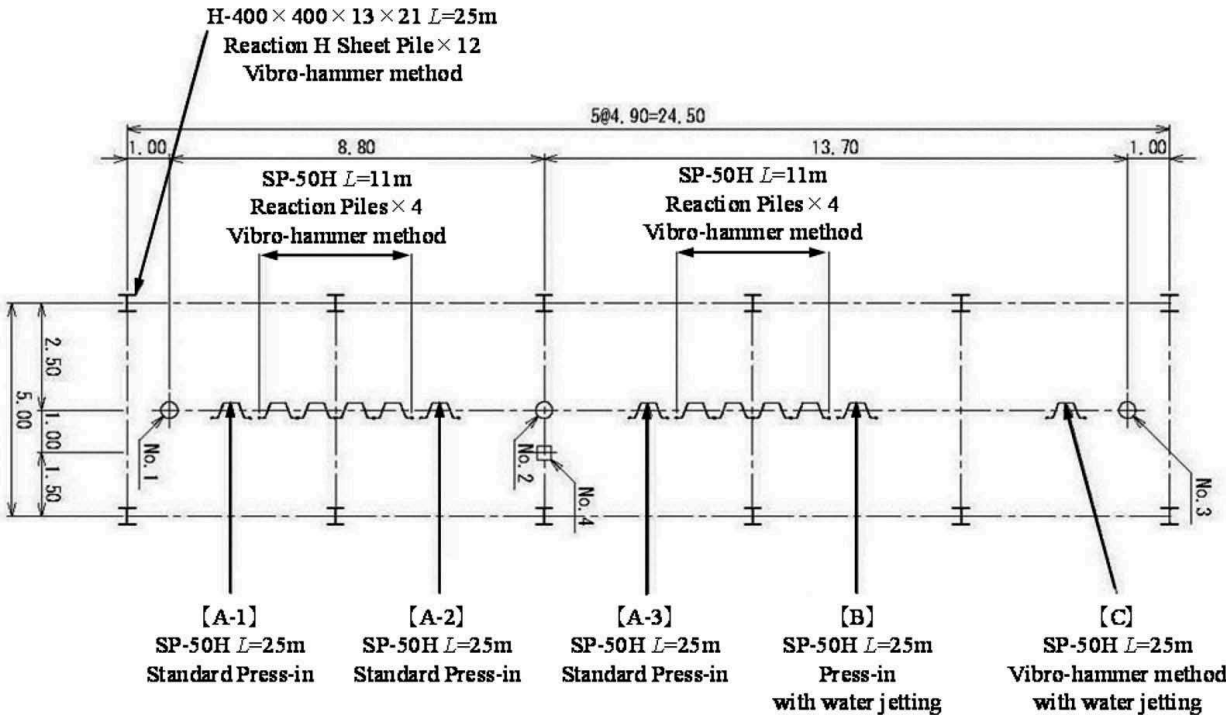

Figure 6. Layout of the field test (Om19 test series) (after Omura *et al*., 2019).

Table 3. Summary of the load test results (Om19 test series).

(a) Capacity

Pile No.	Curing period t_{LT}	Total capacity Q_f [kN]	Base capasity Q_{bf} [kN]	Shaft capasity Q_{sf} [kN]
A-1	14 days	1500	78	1422
A-2	14 days	*	124	*
A-3	14 days	*	117	*

(b) Unit shaft capacity, q_{sf} [kPa]

Gauges No.	① - ②	② - ③	③ - ④	④ - ⑤	⑤ - ⑥
Soil type	sand	sand	silt	silt	silt
N value	10.5	4.8	3.6	4.8	3.3
A-1	21.8	7.6	22.0	30.6	25.5
A-2	*	*	14.5	24.4	27.0
A-3	*	*	40.4	37.5	15.4

* Data not indicated in Omura *et al*., 2019

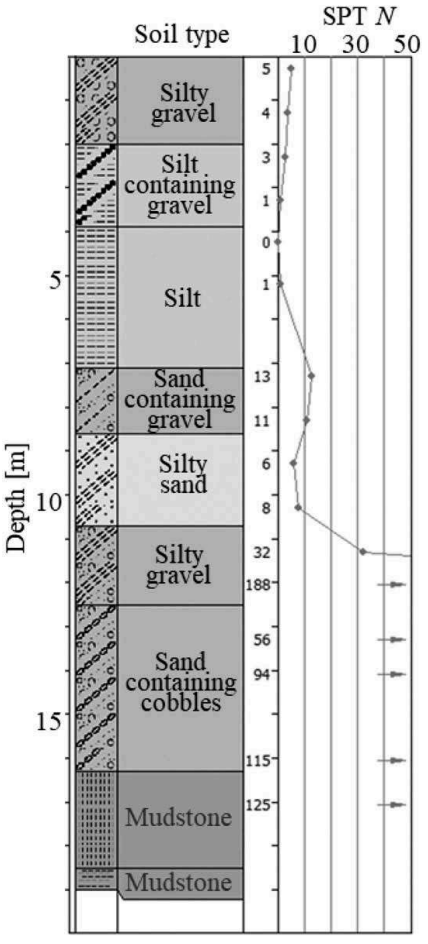

Figure 7. Site soil profile (Eg21 test series) (after Eguchi *et al*., 2021).

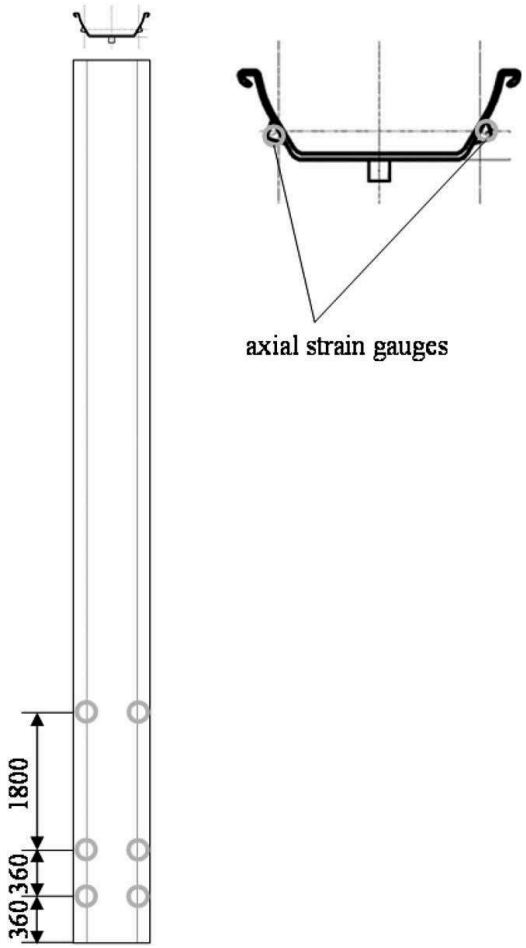

Figure 8. Distribution of strain gauges (Eg21 test series).

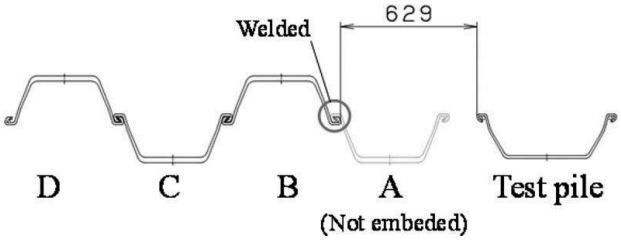

Figure 9. Layout of the field test (Eg21 test series).

Table 4. Press-in conditions (Om19 test series).

z [m]	l_d [mm]	l_u [mm]	v_d [mm]	v_u [mm]	Q'_{UL} [KN]	Memo
0~5	400	200	160	122	200	
5~6.35	400	200	160	122	300	
6.35~6.4	400	200	67	-	300	No extraction

z : Depth
l_d : Displacement of penetration in each cycle of surging
l_u : Displacement of extraction in each cycle of surging
v_d : Penetration velocity in each cycle of surging
v_u : Extraction Velocity in each cycle of surging
Q'_{UL} : Upper – limit of jacking foce

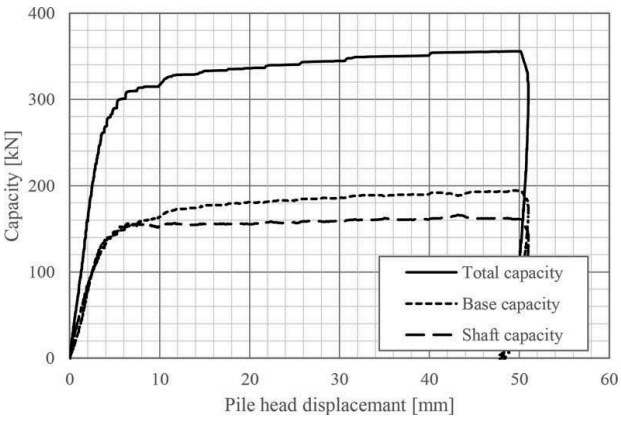

Figure 10. A result of the load displacement curves (Eg21 test series).

Table 5. Summary of the load test results (Eg21 test series).

Curing period t_{LT}	Total capacity Q_f [kN]	Base capasity Q_{bf} [kN]	Shaft capasity Q_{sf} [kN]
20 days	350	189	161

$$q_{sf} = \begin{cases} \min(3\times N, 120) \ \text{[kPa]} \ \text{(for sand)} \\ \min(6\times N, 120) \ \text{[kPa]} \ \text{(for clay)} \end{cases} \quad (7)$$

where P_{sp} is the perimeter of the sheet pile.

3.2 *Adjusting the SPT-based design methods for Standard Press-in*

The two methods introduced in the previous subsection have similar structure in their formulae to estimate Q_{bf} and Q_{sf}. In this section, Eqs. (8) – (11) will be adopted based on these formulae, where N_D is the smallest SPT N value from 0 to 3 meters below the pile base (= N_{D2}), α_b, $\alpha_{s(s)}$ and $\alpha_{s(c)}$ are the coefficients and q_{bf}^{UL}, $q_{sf}^{UL(s)}$ and $q_{sf}^{UL(c)}$ are the upper limits for q_{bf} or q_{sf}. These parameters will be back-analyzed based on the load test results in Om19 test series, as the sheet piles in this test series were highly instrumented and thus the information of measured q_{sf} values at different soil layers are available.

$$Q_{bf} = q_{bf}\times A_{bp} \ (= \text{Eq.}(1)) \quad (8)$$

$$q_{bf} = \min\left(\alpha_b \times N_D,\ q_{bf}^{UL}\right) \ \text{[kPa]} \ (= \text{Eq.}(6)) \quad (9)$$

$$Q_{sf} = \int \left(q_{sf}\times P_{sp}\right) dz \quad (10)$$

$$q_{sf} = \begin{cases} \min\left(\alpha_{s(s)}\times N,\ q_{sf}^{UL(s)}\right) \ \text{[kPa]} \ \text{(for sand)} \\ \min\left(\alpha_{s(c)}\times N,\ q_{sf}^{UL(c)}\right) \ \text{[kPa]} \ \text{(for clay)} \end{cases} \quad (11)$$

Figure 11 shows the correlation between q_{bf} and N_{D2} in Om19 test series, together with the lines

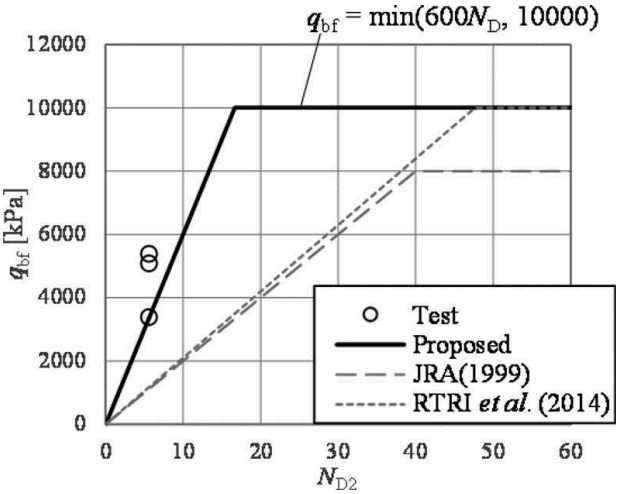

Figure 11. q_{bf} and N_{D2} in Om19 test series and design methods.

determined by each design method. Based on this figure, the α_b value can be determined to be 600 as a lower limit value. It can be confirmed that the existing methods (JRA (1999) and RTRI *et al.* (2014)) provide more than two-fold underestimation in this test series.

Figure 12 shows the correlation between q_{sf} and N in Om19 test series, together with the lines determined by each design method. N was averaged in each soil layer (i.e. for each data plots in this figure). Based on this figure, the $\alpha_{s(s)}$ and $\alpha_{s(c)}$ values can be determined to be 1.9 and 6.6 respectively as average values. It can be confirmed that JRA (1999) provides values comparable to the average of the database and RTRI *et al.* (2014) provides values larger than the average for sand, and vice versa for clay, in this test series.

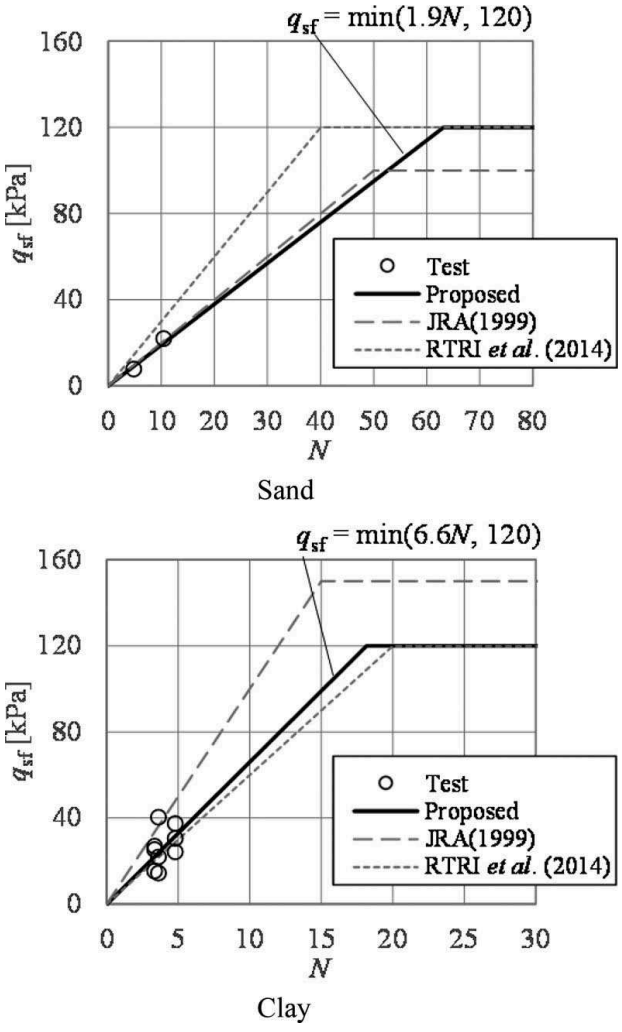

Figure 12. q_{sf} and N in Om19 test series.

Figure 13 shows the comparison of the measured and estimated total capacity (Q_f), Q_{bf} and Q_{sf} for three test series introduced in the previous section. In the estimation, q_{sf} below the depth of the lowest strain gauges (0m, 1m and 0.36m above the pile base in Is20, Om19 and Eg21 test series, respectively) were eliminated. It can be confirmed that the total capacities are safely estimated by all the methods, and that the proposed method provides better estimation than the other two methods for all the three test series. However, the base capacities are significantly underestimated in all the three methods, whereas the shaft capacities are slightly underestimated in the proposed method. One reason for the significant underestimation of Q_{bf} would be the effect of plugging phenomenon in the narrow side of the sheet pile, as pointed out by Taenaka *et al.* (2013). It might be that the sheet piles in Om19 test series were less plugged than those in Is20 and Eg21 test series, leading to smaller back-analyzed α_b value which yields much smaller estimation for Q_{bf} in Is20 and Eg21 test series.

It should be noted that the base displacement to determine the capacity was not consistent in the three test series introduced in Section 2. The base displacement determined based on the definition in Om19 test series (= $0.1W_{sp}$) will be larger than the base displacement determined as one-tenth of the outer diameter of the equivalent tubular pile as adopted in the other two test series (Is20, Eg21), and consequently the capacity determined at $0.1W_{sp}$ will be larger. This paper ignored this effect when analyzing the data in this section. The error caused by this can be judged as being small, being less than 5% in Eg21 test series for example if judged from Figure 10. One reason for this small error might be that the sheet piles in these test series were friction piles, and the resistance (both on base and shaft) did not vary significantly with the base displacement after the yielding point.

4 CONCLUSIONS

Three cases of static vertical load tests on sheet piles installed by Standard Press-in were collected from published sources. An SPT-based design method for the vertical capacity of sheet piles was proposed, by adjusting the existing methods in Japan based on the collected load test results. As a result, the total capacity of the sheet pile was safely estimated if the unit base resistance on the net sectional area was taken as $600N$ in kPa and the unit shaft capacity on the net surface area was taken as $1.9N$ in sandy soil and $6.6N$ in clayey soil. However, the base capacity was significantly underestimated while the shaft capacity was slightly overestimated. The significant underestimation of the base capacity may be due to the effect of the plugging condition of the sheet piles in the field load tests.

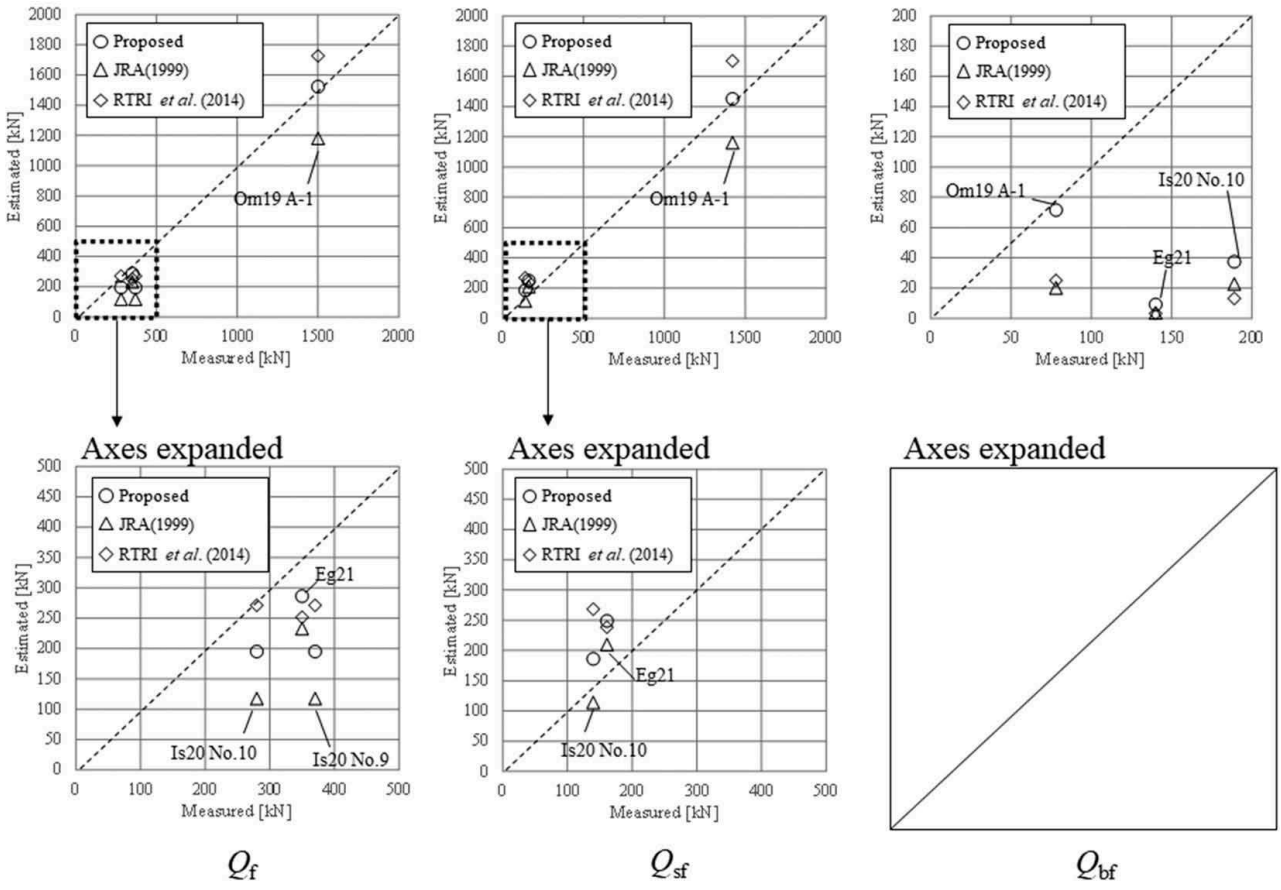

Figure 13. Comparison of measured and estimated capacity.

REFERENCES

International Press-in Association (IPA). 2017. Technical Material on the Use of Piling Data in the Press-in Method, I. Estimation of Subsurface Information, 63p. (in Japanese).

Ishihara, Y., Yasuoka, H. and Shintaku, S. 2020a. Application of Press-in Method to coastal levees in Kochi Coast as countermeasures against liquefaction. *Geotechnical Engineering Journal of the SEAGS & AGSSEA*, 10p.

Ishihara, Y., Ogawa, N., Mori, Y., Haigh, S. and Matsumoto, T. 2020. Simplified static vertical loading test on sheet piles using press-in piling machine. *Japanese Geotechnical Society Special Publication, 8th Japan-China Geotechnical Symposium*, pp. 245–250.

Japan Road Association (JRA). 1999. *Highway Earthwork Series: Manual for Retaining Walls*, 378p.

Kasahara, K., Sanagawa, T., Nishioka, H., Sasaoka, R. and Nakata, Y. 2018. Seismic reinforcement for foundation utilizing sheet piles and soil improvement. *Proceedings of the First International Conference on Press-in Engineering 2018, Kochi*, pp. 555–562.

Kato, I., Hamada, M., Higuchi, S., Kimura, H. and Kimura, Y. 2014. Effectiveness of the sheet pile wall against house subsidence and tilting induced by liquefaction. *Journal of Japan Association for Earthquake Engineering*, 14(4), pp. 4_35-4_49.

Omura, A., Hamaguchi, M., Uetani, O., Oghi, S., Ueda, T., Yokoyama, N. and Osaki, H. 2019. Vertical bearing capacity of sheet-pile by loading tests. *Journal of Japan Society of Civil Engineers, B3 (Ocean Engineering)*, 75(2), pp. I_438-I_443. (in Japanese).

Railway Technical Research Institute (RTRI), Obayashi Corporation, and Nippon Steel & Sumitomo Metal Corporation. 2014. *Design and Construction Manual for Sheet Pile Foundations Applied to Rrailway Structures (draft)*, Version 3, 253p.

Tanaka, K., Kimizu, M., Otani, J. and Nakai, T. 2018. Evaluation of effectiveness of PFS Method using 3D finite element method. *Proceedings of the First International Conference on Press-in Engineering 2018, Kochi*, pp. 209–214.

Taenaka, S. 2013. Development and optimisation of steel piled foundations. *Ph. D. thesis, The University of Western Australia*, 289p.

The Japanese Geotechnical Society (JGS). 2002. Method for static axial compressive load test of single piles. *Standards of Japanese Geotechnical Society for Vertical Load Tests of Piles*, pp. 49–53.